Slow diffusion of hydrogen at a screw dislocation core in α-iron

Hajime Kimizuka* and Shigenobu Ogata

Department of Mechanical Science and Bioengineering, Graduate School of Engineering Science, Osaka University, Osaka 560-8531, Japan

(Received 29 May 2011; published 18 July 2011)

Here we demonstrate and characterize the H-diffusion behavior around a screw dislocation in body-centered cubic (bcc) α-Fe by performing path-integral molecular dynamics modeling and adopting an *ab initio*–based potential. Counterintuitively, our results indicate that the H diffusivity along the dislocation line is significantly lower than lattice diffusion. Thus, the "fast" pipe diffusion does not occur for H in α-Fe.

DOI: 10.1103/PhysRevB.84.024116 PACS number(s): 66.30.jp, 02.70.Ns, 61.72.Lk

I. INTRODUCTION

Understanding the H diffusion and transport in Fe and Fe alloys is extremely important because H severely degrades ductility and causes H embrittlement, which has been a serious materials problem. Numerous experimental studies have been performed on H diffusivity in Fe (for reviews, see Refs. 1 and 2), and the H diffusion was found to be significantly suppressed with increasing dislocation density in the specimens[3]; however, there is still no consensus on the details about the fundamental mechanism of H diffusion around dislocations. Interstitial atom migration in crystalline metals is widely believed to be more rapid along the dislocation than through the regular lattice, since the free volume of the dislocation core regions is greater than that of the lattice. Such a transport phenomenon is known as "pipe diffusion" (for examples, see Refs. 4 and 5). Theoretical approaches based on classical molecular mechanics and/or molecular dynamics have been used to study the H trapping and migration around a dislocation in Fe.[6–10] Because H is a light element, the intrinsic processes in H diffusion are expected to be strongly influenced by the quantum behavior of H. However, to our knowledge, the nuclear quantum effects at finite temperatures have not been considered in studies on H diffusion around dislocations.

In this study, we investigate the H diffusivity and the H trappability (trapping effect) from free-energy surfaces around a screw dislocation in α-Fe. We also investigate the atomic trajectories of trapped H around the dislocation at finite temperatures. We predicted these properties and behaviors by performing path-integral molecular dynamics modeling based on first principles; in our calculations, we took quantum effects into consideration.

II. METHODS

A. *Ab initio*–based analytical potential for the Fe-H system

In the previous study, we constructed an interatomic potential for the Fe-H system within the embedded-atom-method (EAM) formalism.[11,12] We developed this potential for specific use in path-integral simulations, and confirmed that this potential model gives accurate and reliable results for H diffusivity in a regular α-Fe lattice (bcc structure) over a wide temperature range.[11] To apply this model to the study of the defect trapping of H in Fe, new parameters were determined.

The energy of a system is defined in accordance with the EAM scheme:

$$E = \frac{1}{2}\sum_{j\neq i}^{N}\phi_{ij}(r_{ij}) + \sum_{i}^{N}F_i(\bar{\rho}_i), \tag{1}$$

where r_{ij} is the distance between atoms i and j, and ϕ_{ij} is the two-body part of the potential between atoms i and j. F_i is the embedding energy and $\bar{\rho}_i$ is the electron density at atom i due to the remaining atoms in the system. The density $\bar{\rho}_i$ is defined as

$$\bar{\rho}_i = \sum_{j\neq i}^{N}\rho_j(r_{ij}), \tag{2}$$

where ρ_j is the electron density contributed by atom j. The present potential for the Fe-H system consists of seven functions: ϕ_{FeFe}, ϕ_{HH}, ϕ_{FeH}, F_{Fe}, F_{H}, ρ_{Fe}, and ρ_{H}. In this model, interactions between pure elements are represented by existing EAM potentials. The form of ϕ_{FeFe}, F_{Fe}, and ρ_{Fe} for Fe is predetermined on the basis of the studies conducted by Mendelev *et al.*[13] Here, the same parameters as those in potential 2 (in Ref. 13) were employed, but the sign of the parameter a_7^{φ} was changed from positive to negative. For the functions ϕ_{HH}, F_{H}, and ρ_{H}, we used the model developed by Angelo *et al.*,[14] in which the parameters were corrected by Baskes *et al.*[15]

The remaining pair interaction ϕ_{FeH} is described by the Morse function as

$$\phi_{\mathrm{FeH}}(r) = \alpha_1[e^{-2\alpha_2(r-\alpha_3)} - 2e^{-\alpha_2(r-\alpha_3)}], \tag{3}$$

where α_1, α_2, and α_3 are fitting parameters. To develop the EAM potential for the Fe-H system, F_{H} was modified so that the total H energy is not affected. The form of the modification is

$$\rho_{\mathrm{H}} = S_{\mathrm{H}}\rho_{\mathrm{H}}, \tag{4}$$

$$F_{\mathrm{H}}(\bar{\rho}) = F_{\mathrm{H}}(\bar{\rho}/S_{\mathrm{H}}), \tag{5}$$

where S_{H} is the relative scaling factor for ρ_{H}. A linear term was added to ϕ_{FeH} to provide a smooth cutoff at the cutoff distance r_c. This term is given by

$$\phi(r) = \phi_{\mathrm{FeH}} + a(r - r_c) + b, \tag{6}$$

where $a = -\phi'_{\mathrm{FeH}}(r_c)$ and $b = -\phi_{\mathrm{FeH}}(r_c)$. The parameters S_H and α_i were fitted to reproduce not only the activation barrier at the transition state for H migration in a regular lattice but also

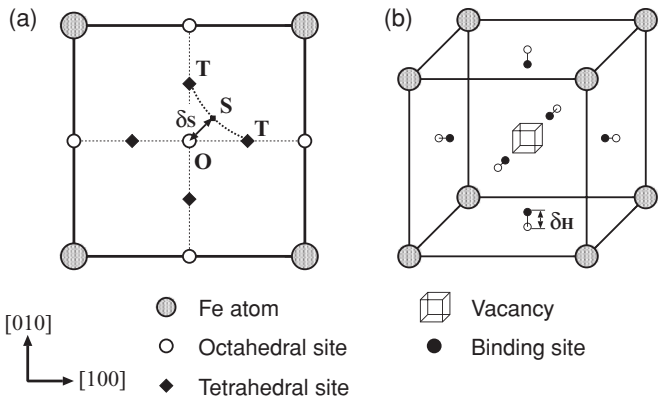

FIG. 1. Schematic illustration of interstitial and vacancy-binding sites for H atoms in Fe: (a) Positions of T-sites and O-sites on the (001) plane of the bcc Fe lattice. The S-site is the saddle point along the MEP for direct hopping of a H atom between two neighboring T-sites. (b) H-binding sites at a vacancy. The binding site is displaced from the O-site toward the vacancy by δ_H.

the binding state of a H atom to a vacancy, where the energy and geometry of each state are obtained from the spin-polarized density functional theory (DFT) calculations presented in the literature.[17,18]

The minimum energy path (MEP) and the transition state between two adjacent tetrahedral sites (T-sites) for the EAM potential are identified by using the nudged elastic band method[16] with an $Fe_{128}H$ supercell ($4 \times 4 \times 4$ unit cells). As shown in Fig. 1, the S-site, which is the saddle point for the relaxed potential energy surface, is located in the vicinity of the midpoint between the two neighboring T-sites, at a distance δ_S from the octahedral site (O-site). The parameters are optimized to represent the migration energy (the energy barrier along the MEP) E_m, the distance between the O-site and S-site δ_S, the difference between the energies of the H atom at the O-site and the T-site $E_{T\text{-}O}$, the binding energy of a single H atom to a monovacancy E_{VH}, and the displacement of the H atom from the O-site toward the vacancy δ_H (Fig. 1). Here, the target values for the optimization are obtained from the spin-polarized DFT calculations presented in the literature.[17,18] The zero-point energy (ZPE) contributions are excluded while calculating these energy values. Therefore, the present analytic potential model describes the *ab initio*–based "bare" (not ZPE-corrected) potential energy surface for the Fe-H system. Table I lists the calculated values of E_m, δ_S, $E_{T\text{-}O}$, E_{VH}, and δ_H, together with the results obtained for the potential developed by Wen *et al.*[6] We can confirm that our potential can reproduce the DFT energy differences among the T-site, S-site, and O-site, where a H atom may reside. In addition, this model gives accurate values of E_{VH} and δ_H. The obtained parameters for ϕ_{FeH} are listed in Table II.

B. Evaluation of the PIMD-based free-energy profiles

To characterize the *apparent* activation free energies for H diffusion across and along the dislocation line at finite temperatures, we evaluated the differences between the free energies of the system ΔF for H at the interstitial or binding sites using the path-integral molecular dynamics (PIMD) method.[19] We

TABLE I. Calculated values of the migration energy (E_m), distance between the O-site and S-site (δ_S), the difference between the energies of the H atoms ($E_{T\text{-}O} = E_O - E_T$) at the O-site and T-site, the binding energy of a single H atom to a monovacancy E_{VH}, and the displacement of the H atom from the O-site toward the vacancy δ_H. The target DFT energies in the literature[17,18] are not ZPE-corrected values.

		DFT	Our Model	Wen
E_m	(eV)	0.088[a]	0.088	0.029
δ_S	(Å)	0.407[a]	0.407	0.217
$E_{T\text{-}O}$	(eV)	0.13[a]	0.142	0.035
E_{VH}	(eV)	0.50[b]	0.402	0.58[c]
δ_H	(Å)	0.224[b]	0.233	0.39[c]

[a]Reference 17.
[b]Reference 18.
[c]Reference 6.

simulated the classical isomorph by a molecular dynamics method, and calculated the static averages (e.g., mean forces and spatial distributions) by sampling configurations of the system using statistical weights. The system consists of cyclic chains of beads (P beads on each chain) coupled by harmonic springs.[20] The spring constant of the chains is $mP/(\beta\hbar)^2$. Here, m represents the mass of the quantum particles, β is the inverse temperature $(k_BT)^{-1}$, k_B is the Boltzmann constant, and $\hbar$ is the Planck constant. The isomorphism becomes exact in the limit $P \to \infty$. In this analysis, we treated all atoms quantum-mechanically by discretizing the path into $P = 64$ imaginary time slices. To carry out the PIMD calculations at a desired temperature, massive Nosé-Hoover chains[21] were attached to normal-mode coordinates of the system.[22] The mean force acting on each of the centroids of the quantum particles was then calculated to evaluate ΔF within the canonical ensemble for a 10-ps run. In all calculations, the time step was 0.1 fs.

The free-energy profiles for H migration based on the PIMD were evaluated as follows: First, the minimum energy path and the transition state for H diffusion in α-Fe were obtained by using the nudged elastic band method[16] in the classical regime. An interpolated chain of configurations (images) between the initial and final positions (i.e., neighboring trapping sites) was connected by springs and simultaneously relaxed so that it becomes the minimum energy path. Each of the obtained images along the minimum energy path is supposed to correspond to the centroid configuration $\boldsymbol{R}$ of the quantum chains. Then, the mean force $\langle \boldsymbol{F}(\boldsymbol{R}) \rangle_{PI}$ was calculated in the

TABLE II. Parameters for the mixed two-body potential ϕ_{FeH}.

Parameter	ϕ_{FeH}
S_H	16.0
α_1 (eV)	0.472
α_2 (Å^{-1})	4.42
α_3 (Å)	1.57
a (10^{-5} eV/Å)	−3.73156
b (10^{-6} eV)	8.44249
r_c (Å)	4.2

canonical ensemble with fixed centroid positions; here, $\boldsymbol{F}(\boldsymbol{R})$ is the force acting on the quantum chain when the centroids are located at $\boldsymbol{R}$, and the quantities in brackets are path-integral average values. The difference between the free energies of the system ΔF was evaluated by integrating the mean force along the diffusion path $\boldsymbol{S}$, i.e., $\Delta F = -\int d\boldsymbol{S} \cdot \langle \boldsymbol{F}(\boldsymbol{R}) \rangle_{\mathrm{PI}}$ (Refs. 11 and 23).

III. RESULTS AND DISCUSSION

A. H-vacancy binding free energy

To check the validity of our potential model, we evaluated the apparent H-vacancy binding free energy (ΔF for a H atom at the binding site and regular T-site) from the PIMD-based free-energy profiles around a monovacancy in α-Fe. At an ambient temperature of 300 K, the value calculated while taking quantum effects into consideration is 0.64 eV. As mentioned in Table I, the classical limit of E_{VH} is set to 0.40 eV for our potential; thus, it is clear that the calculated binding free energy for H at a vacancy increases when quantum effects are taken into account. Further, since the corresponding experimental value in the literature is 0.63 eV (Ref. 24) and the ZPE-corrected DFT values are 0.56 eV (Ref. 18) and 0.69 eV (Ref. 10), we confirm that our potential can give accurate results for the energetics of H trapping by defects. Thus we used the present model in the following path-integral analysis for the dislocation trapping of H.

B. Trapping and migration of H at a screw dislocation

We considered the binding behavior of a single H atom at an $a_0/2\langle 111\rangle$ screw dislocation. To calculate the PIMD-based free-energy profiles around the screw dislocation, we selected the triclinic 1155-atom supercell containing a pair of screw dislocation cores with a sixfold symmetric structure in the $(1\bar{1}0)\langle 111\rangle$ slip system.[25] We define the configuration of our model as follows: $\boldsymbol{e}_1 = a_0[11\bar{2}]$, $\boldsymbol{e}_2 = a_0[1\bar{1}0]$, and $\boldsymbol{e}_3 = a_0/2[111]$, where $a_0 = 2.8553$ Å. Two equally spaced screw dislocations are included in order to form a dipole in a periodically repeated supercell with three edges: $\boldsymbol{h}_1 = 7\boldsymbol{e}_1$, $\boldsymbol{h}_2 = 3.5\boldsymbol{e}_1 + 5.5\boldsymbol{e}_2 + 0.5\boldsymbol{e}_3$, and $\boldsymbol{h}_3 = 5\boldsymbol{e}_3$, at a dipole separation $\boldsymbol{d} = \boldsymbol{h}_1/2$. We obtained the MEP for H diffusion between interstitial sites by using the nudged elastic band method,[16] and then, we evaluated ΔF for H at temperatures of 300 and 1000 K along the slip plane from the dislocation core to the regular lattice region and along the [111] direction parallel to the dislocation line.

Figure 2 shows the PIMD-based free-energy profiles for H diffusion around a screw dislocation. We can confirm that the H atom is strongly trapped in the vicinity of the dislocation core; the PIMD-based values of the maximum binding free energy for H around a screw dislocation are 0.20 eV at 1000 K and 0.29 eV at 300 K (at the α-site), while its classical limit is 0.13 eV. Thus, as the temperature decreases, the binding free energy at a dislocation is enhanced by the quantum effects, as in the case of a vacancy. In addition, the diffusion barrier for H close to a dislocation remarkably increases as the temperature decreases, while that in the regular lattice region decreases[11]; the maximum diffusion barrier for escaping from the binding

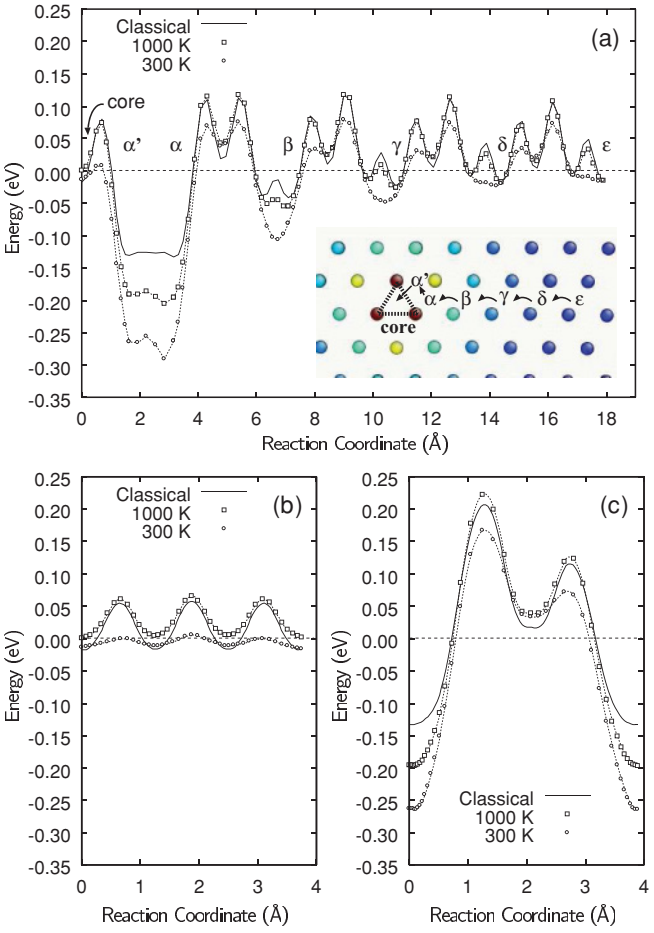

FIG. 2. (Color online) Free-energy profiles for H-atom diffusion around a screw dislocation: (a) diffusion along the {110} slip plane, (b) diffusion through the core along the [111] direction (parallel to a dislocation line), and (c) diffusion through the binding site (α-site) along the [111] direction. Here, the Greek letters (α, β, etc.) represent the stable H-binding sites on the slip plane. In the inset of (a), the Fe atoms are colored according to their local von Mises shear strain invariant with a red-green-blue (RGB) color ramp; blue (darkest grey far from the core) and red (darkest grey near the core) correspond to the lowest (0.0) and highest (0.1265) values, respectively.

site, as calculated by PIMD, is 0.36 eV at 300 K. Further, as in Fig. 2(c), there is a high barrier for diffusion of a H atom through the binding site (α-site) along the [111] direction (parallel to the dislocation line); the activation free energy is 0.43 eV at 300 K. On the other hand, the barrier for diffusion through a dislocation core, i.e., 0.022 eV at 300 K, is found to be significantly lower than that in the regular lattice region [Fig. 2(b)]. However, from the free-energy profiles across the dislocation [Fig. 2(a)], we can confirm that the state of a H atom in the core is energetically unstable at finite temperatures, and a H atom can easily leave the core for the nearest binding sites. These results indicate that there is a high barrier for H diffusion both across and along the screw dislocation, and this results in very low diffusivity compared to that in the regular lattice region.

Many of the experimental values of the binding energies between H and the dislocation range from 0.21 to 0.31 eV, and some are in the range 0.50–0.62 eV (for example, see

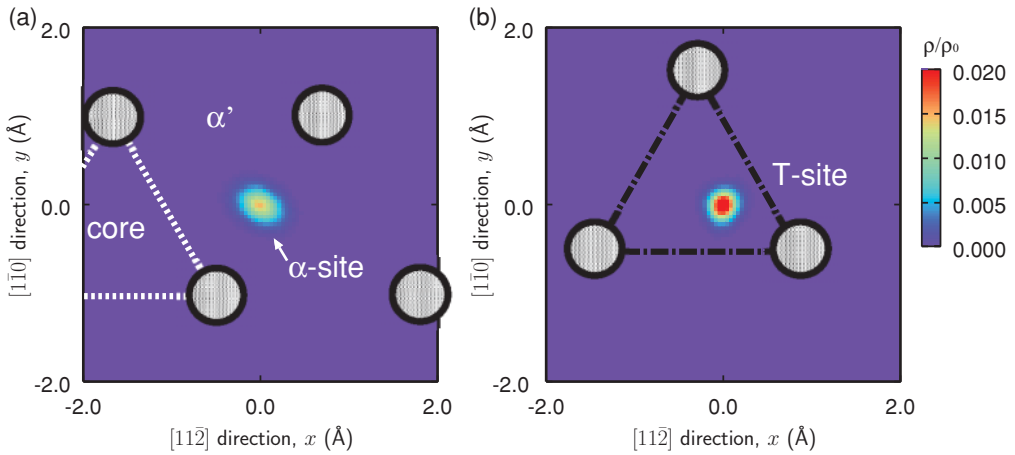

FIG. 3. (Color online) Quantum distribution of a H atom at 300 K: The results are shown for the case in which the centroid of the H atom is located at the (a) binding site (α-site) near the dislocation core and (b) T-site in the regular Fe lattice. The circles represent the equilibrium positions of the Fe atoms.

Refs. 3 and 26). The results of these estimations largely depend on the models employed, and they cannot be used to clearly distinguish between edge and screw dislocations. Although these experimental values should be regarded as tentative, the values we predicted for the binding free energy lie in the experimental range.

C. H-binding state at a screw dislocation

To investigate the binding state, we examined the quantum distributions of a H atom at the maximum binding site (α-site) near the core (Fig. 3). For comparison, we plotted the result at the minimum energy site (T-site) in the regular lattice. In thermal equilibrium, the springs in the cyclic chain have some mean extension, and the chain as a whole therefore spreads out. The size of the chain at a certain temperature is determined by the curvature of the potential well in which the particle is confined.[27] We found that the H-atom distribution at the α-site broadens and spreads out toward the adjacent binding site (α'-site) at 300 K, while the distribution at the T-site is rather narrow and isotropic. This suggests that the potential energy surface for the binding-site configuration has a smaller curvature (i.e., lower vibrational energy) than that for the regular T-site configuration, as is also inferred from Fig. 2(a). Thus, the significant enhancement of H binding due to quantum effects results from the large delocalization of the H atom in the binding-site configuration compared to the confinement of the H atom in the T-site configuration. With increasing temperature, such a delocalization effect becomes negligible because of the rapid contraction of the quantum chain. Therefore, the difference between the free energies for a H atom at the binding site and T-site significantly decreases and approaches its classical limit as the temperature increases [Fig. 2(a)].

D. H diffusion around a screw dislocation

To confirm the change in H diffusivity in the vicinity of a screw dislocation, centroid path-integral molecular dynamics[22] was adopted. Here, the centroids of the isomorphic beads of a quantum particle evolve in real time according to an instantaneous force, which in turn is generated according to an on-the-fly scheme.[22] To carry out the calculations, an additional Nosé-Hoover thermostat[28] was attached to the centroid coordinates. A H atom was initially placed at one of the interstitial sites inside the dislocation core, and then, the trajectory for the centroid of a H atom was evaluated at 300 K within the canonical ensemble for a 0.3-ns run (Fig. 4).

As shown in Fig. 4, the H trajectory is more strongly confined to the region around the core than the H trajectory in the regular lattice region. The H atom, which was initially placed inside the core, immediately moves to the nearest binding site and continues to jump between adjacent binding sites near the core (α'- and α-sites); thus, no significant diffusion is observed both across and along the dislocation. To measure the spread of the H trajectory, the square root values of the second moment of the H distribution, $R = \langle \Delta \boldsymbol{r}^2 \rangle^{1/2}$, were evaluated during a 0.3-ns run, where $\Delta \boldsymbol{r}$ represents the displacement of the H centroid from the center of the distribution. We found that the value of R around the screw dislocation is 0.66 Å, while that in the regular lattice region is 14.2 Å. This clearly indicates that the H diffusivity decreased considerably in the region close to the screw dislocation core, because of the strong influence of the rugged free-energy surface around the dislocation.

IV. CONCLUSIONS

We show that the H atom is strongly trapped in the vicinity of the screw dislocation, and there is a high barrier for H diffusion both across and along the dislocation; thus the dislocation lines do not act as fast pathways for H diffusion in α-Fe. In this paper, we focused on a pure screw dislocation that has the least amount of free volume of all types of dislocations in α-Fe. It is noteworthy that, even in the case of an edge dislocation, we find no low-energy pathway for H diffusion parallel to the dislocation line (see the Appendix). Since the apparent migration free energy for H in the regular lattice region (i.e., diffusion barrier along the path from a T-site

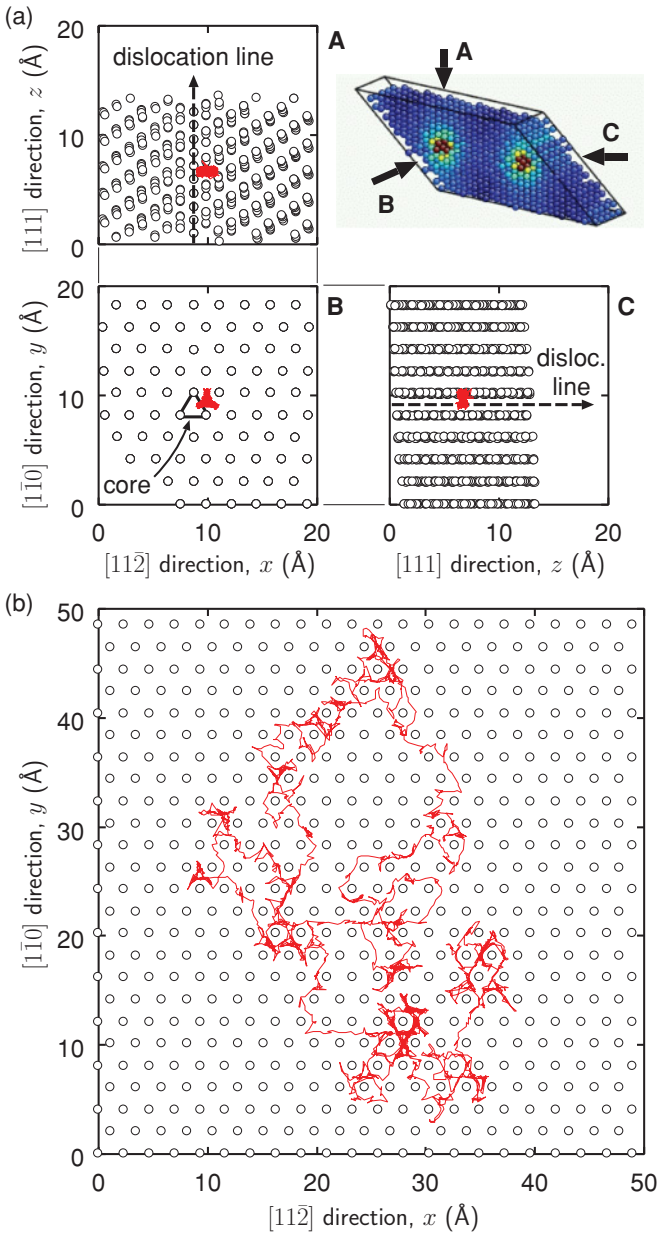

FIG. 4. (Color online) Trajectories of a H atom: (a) trajectories around the screw dislocation and (b) trajectories in the regular α-Fe lattice for 0.3 ns at 300 K.

to an S-site), as calculated by PIMD, is 0.034 eV at 300 K for the present potential model, the activation free energy for H diffusion close to the dislocations is estimated to be 11–13 times higher than that in the regular lattice region at the ambient temperature. Therefore, the dislocation pipe diffusion of H results in significantly lower diffusivity than the lattice diffusion. In other words, the diffusivity resulting from dislocation pipe diffusion is 10^4–10^5 times lower than that resulting from lattice diffusion.

ACKNOWLEDGMENTS

The authors would like to thank K. Takai, M. Itakura, and H. Mori for useful discussions. This study was partially supported by Grants-in-Aid for Young Scientists (B), No. 21760077, Scientific Research (A), No. 23246025, Scientific Research on Innovative Area, No. 22102003, and Challenging Exploratory Research, No. 22656030.

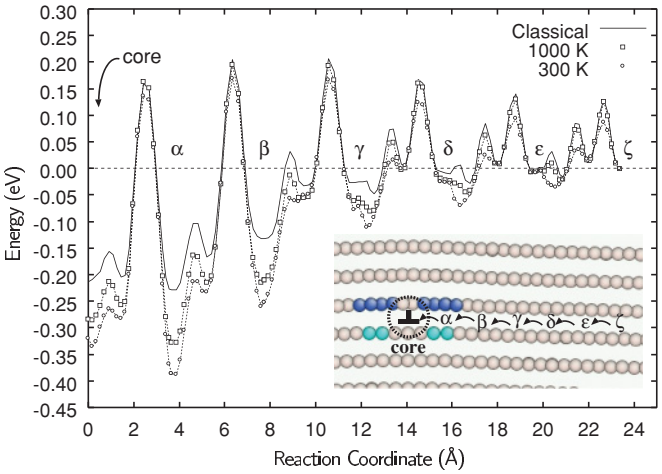

FIG. 5. (Color online) Free-energy profiles for H-atom diffusion along the {110} slip plane of an edge dislocation. The Greek letters (α, β, etc.) represent the stable H-binding sites on the slip plane. In the inset, the Fe atoms are colored according to their coordination numbers [blue (darkest grey), 13; white (lightest grey), 14; cyan (mid-dark grey), 15].

APPENDIX: TRAPPING AND MIGRATION OF HYDROGEN AT AN EDGE DISLOCATION

We consider the binding behavior of a single H atom at an $a_0/2\langle 111\rangle\{110\}$ edge dislocation. We employed an orthogonal supercell containing 3960 atoms with three edges: $\boldsymbol{h}_1 = 14a_0[111]$, $\boldsymbol{h}_2 = 12a_0[1\bar{1}0]$, $\boldsymbol{h}_3 = 2a_0[11\bar{2}]$. The dislocation is introduced into the center of the block according to its anisotropic elastic displacement fields. The periodic boundary condition is applied along the $\boldsymbol{h}_3$, while free boundary conditions are imposed along the $\boldsymbol{h}_1$ and $\boldsymbol{h}_2$. We obtained the minimum energy path for H diffusion from the dislocation core to the regular lattice region along the slip plane, and then evaluated ΔF for H at temperatures of 300 and 1000 K.

Figure 5 shows the PIMD-based free energy profiles for H diffusion around an edge dislocation. As in a screw dislocation, the binding free energy at an edge dislocation is enhanced by the quantum effects as temperature decreases; the PIMD-based values of the maximum binding free energy for H around an edge dislocation are evaluated as 0.33 eV at 1000 K and 0.39 eV at 300 K, respectively, while its classical limit is 0.23 eV. Also, the maximum diffusion barrier to escape from the binding site is calculated as 0.56 eV at 300 K. Thus the diffusion barrier for H close to a dislocation remarkably increases as temperature decreases. Similarly, we find that there is no low-energy pathway for H diffusion along the $[11\bar{2}]$ direction parallel to dislocation line. This indicates that the H diffusivity is slowed down close to the edge dislocation core both across and along the dislocation line, when the motion of dislocations is sufficiently slow compared to the diffusion of H.

*kimizuka@me.es.osaka-u.ac.jp

[1] J. Völkl and G. Alefeld, in *Hydrogen in Metals I: Basic Properties*, edited by G. Alefeld and J. Völkl (Springer, Berlin, 1978), p. 321.
[2] K. Kiuchi and R. B. McLellan, Acta Metall. **31**, 961 (1983).
[3] H. Hagi and Y. Hayashi, Trans. Jpn. Inst. Met. **28**, 368 (1987); **28**, 375 (1987).
[4] H. Mehrer, *Diffusion in Solids: Fundamentals, Methods, Materials, Diffusion-Controlled Processes* (Springer, Berlin, 2007), p. 547.
[5] M. Legros, G. Dehm, E. Arzt, and T. J. Balk, Science **319**, 1646 (2008).
[6] M. Wen, X.-J. Xu, S. Fukuyama, and K. Yokogawa, J. Mater. Res. **16**, 3496 (2001).
[7] M. Wen, S. Fukuyama, and K. Yokogawa, Acta Mater. **51**, 1767 (2003).
[8] B.-J. Lee and J.-W. Jang, Acta Mater. **55**, 6779 (2007).
[9] S. Taketomi, R. Matsumoto, and N. Miyazaki, Acta Mater. **56**, 3761 (2008).
[10] A. Ramasubramaniam, M. Itakura, and E. A. Carter, Phys. Rev. B **79**, 174101 (2009).
[11] H. Kimizuka, H. Mori, and S. Ogata, Phys. Rev. B **83**, 094110 (2011).
[12] H. Kimizuka, H. Mori, H. Ushida, and S. Ogata, J. Jpn. Inst. Met. **73**, 571 (2009).
[13] M. I. Mendelev, S. Han, D. J. Srolovitz, G. J. Ackland, D. Y. Sun, and M. Asta, Philos. Mag. **83**, 3977 (2003).
[14] J. E. Angelo, N. R. Moody, and M. I. Baskes, Modell. Simul. Mater. Sci. Eng. **3**, 289 (1995).
[15] M. I. Baskes, X. Sha, J. E. Angelo, and N. R. Moody, Modell. Simul. Mater. Sci. Eng. **5**, 651 (1997).
[16] H. Jónsson, G. Mills, and K. W. Jacobsen, in *Classical and Quantum Dynamics in Condensed Phase Simulations*, edited by B. J. Berne, G. Ciccotti, and D. F. Coker (World Scientific, Singapore, 1998), p. 385.
[17] D. E. Jiang and E. A. Carter, Phys. Rev. B **70**, 064102 (2004).
[18] Y. Tateyama and T. Ohno, Phys. Rev. B **67**, 174105 (2003).
[19] M. E. Tuckerman, in *Quantum Simulations of Complex Many-Body Systems: From Theory to Algorithms*, edited by J. Grotendorst, D. Marx, and A. Muramatsu (John von Neumann Institute for Computing, Jülich, 2002), p. 269.
[20] R. P. Feynman and A. R. Hibbs, *Quantum Mechanics and Path Integrals* (McGraw-Hill, New York, 1965).
[21] D. J. Tobias, G. J. Martyna, and M. L. Klein, J. Phys. Chem. **97**, 12959 (1993).
[22] J. Cao and G. A. Voth, J. Chem. Phys. **99**, 10070 (1993); **101**, 6168 (1994).
[23] M. J. Gillan, Phys. Rev. Lett. **58**, 563 (1987).
[24] F. Besenbacher, S. M. Myers, P. Nordlander, and J. K. Nørskov, J. Appl. Phys. **61**, 1788 (1987).
[25] J. Li, C.-Z. Wang, J.-P. Chang, W. Cai, V. V. Bulatov, K.-M. Ho, and S. Yip, Phys. Rev. B **70**, 104113 (2004).
[26] J. P. Hirth, Metall. Trans. A **11A**, 861 (1980).
[27] M. J. Gillan, in *Computer Modelling of Fluids, Polymers and Solids*, edited by C. R. A. Catlow, S. C. Parker, and M. P. Allen (Kluwer, Dordrecht, 1990), p. 155.
[28] S. Nosé, Mol. Phys. **52**, 255 (1984); W. G. Hoover, Phys. Rev. A **31**, 1695 (1985).